Convolution Surfaces based on Polygonal Curve Skeletons

Evelyne Hubert, Marie-Paule Cani

Convolution Surfaces based on Polygonal Curve Skeletons

Evelyne Hubert [a]

[a] *INRIA Sophia Antipolis, France*

Marie-Paule Cani [b]

[b] *Laboratoire Jean Kuntzmann (Grenoble University, CNRS) and INRIA Grenoble-Rhône-Alpes, France*

Abstract

This paper reviews and generalizes *Convolution Surfaces*, a technique used in Computer Graphics to generate smooth 3D volumes around *skeletons* that are lower dimensional or simpler geometric models of the shape to be created. Convolution surfaces are defined as level sets of a function obtained by integrating a kernel function along this skeleton. To allow interactive modeling, the technique has relied on closed form formulae for integration obtained through symbolic computation software.

This paper provides new qualitative results and generalizations on the topic when the skeleton is a polygonal line. It is also an opportunity for us to introduce the field of convolution surfaces to the symbolic computation community, hoping that researchers well versed into integration techniques can bring additional contributions to this appealing shape representation.

Key words: Integration, Recurrences, Geometric Modelling, Computer Graphics
1991 MSC: 44-04 39A60 68U05

1 Introduction

This paper studies Convolution Surfaces, a class of implicit surfaces that was introduced in Computer Graphics. They are the boundaries of smooth vol-

Email addresses: evelyne.hubert@sophia.inria.fr (Evelyne Hubert), Marie-Paule.Cani@inrialpes.fr (Marie-Paule Cani).
URLs: www.inria.fr/cafe/Evelyne.Hubert (Evelyne Hubert), www-evasion.imag.fr/Membres/Marie-Paule.Cani (Marie-Paule Cani).

umes around a graph of geometric elements (such as points, line segments, polygons), thus offering intuitive shape control thanks to a *skeleton plus radius* abstraction. In addition to analyzing in depth existing techniques related to convolution surfaces generated by skeleton curves, this paper presents a set of results and generalizations that should contribute to extend the impact of convolution surfaces in Computer Graphics.

Efficiently computing convolution surfaces relies on the closed form formulae for integration obtained through symbolic computation software. After differentiation, the topic of integration was among the first problems addressed by symbolic integration. Based on the work of Abel and Liouville in the nineteenth century, integration in finite terms was an active area of research, from both the mathematical and computer perspective in the twentieth century up to its textbook form today (Geddes et al., 1992) and in depth study (Bronstein, 2005). In consequence, we found it relevant to report to the symbolic computation community on the successful application of integration for computer graphics. We hope that this brings further contributions to the topic.

Finding geometric representations that ease the interactive modeling and animation of free-form 3D shapes has long been a major challenge for the computer graphics community. While only parametric surfaces were used at first, the idea of using iso-surfaces (level set) of a scalar field (function), defined from the distance to skeletal points, was first introduced by Blinn (1982) in the eighties. The use of the Gaussian function there was soon followed by the introduction of piecewise polynomial functions with compact support leading to implicit representations called metaballs (Nishimura et al., 1985) and soft objects (Wyvill et al., 1986). These representations were appealing, for both geometric shape modeling and computer animation, because the embedded skeleton offered intuitive shape control, while summing the fields generated by all the points enabled to smoothly blend different components into a single, complex shape.

Using more complex skeletons such as graphs of line segments or triangles was a natural extension of these first models, with the appeal of offering an independent control of the shape topology (through the skeleton) and geometry (through its thickness around it). However, summing the fields, as given by decreasing functions of the distance, generated by the different skeletal elements created bulges at joints. Therefore, Bloomenthal and Shoemake (1991) introduced Convolution Surfaces with the idea that the integral of a kernel function over the skeleton is independent on the number of pieces in which this latter is cut into. The resulting isosurface presents then no bulge at junctions.

The use of numerical integration of Bloomenthal and Shoemake (1991) to evaluate the convolution integral for a Gaussian kernel was considered a major problem for both accuracy and efficiency. Consequently McCormack and Sherstyuk (1998) introduced the so called Cauchy kernel to provide analytical solutions for the convolution integral for skeletons consisting of line segments,

arcs of circles, and triangles. Sherstyuk (1999b) compared the efficiency of different kernels either given as piecewise polynomial functions with compact supports or decreasing function of the distance with infinite support - such as the Cauchy kernel and some power inverse kernels. The cubic power inverse was later introduced by (Cani and Hornus, 2001) and proved more efficient in the latter category.

In the case of 1-dimensional skeleton, these models would create tubular shapes with a rather constant thickness along the skeletal elements, thus restricting the set of modeled shapes. A first strategy to make the thickness of the volume around the skeleton vary was to post-mutiply the convolution function by a shaping function (Sherstyuk, 1999a; Cani and Hornus, 2001; Angelidis and Cani, 2002). Smoother surfaces were then obtained by Jin et al. (2001); Jin and Tai (2002a) and Hornus et al. (2003) by introducing a *weight* function under the integral sign. On one hand Hornus et al. (2003) used linearly varying weight along each skeletal element while enabling to increase the number of these elements through a subdivision mechanism. On the other hand Jin et al. (2001); Jin and Tai (2002a) used polynomial functions of degree up to 3 as weights thus enabling the use of much less skeletal elements for shapes with contour that can be sketched with cubic Bezier curves.

All these different contributions heavily relied on closed form expressions for the convolution integrals. Hidden behind those results was the use of symbolic computation software, showing the success of this branch of symbolic computation. However, these results were independently computed for each different kernel function without any unified, well formulated strategy on the way to use this kind of software. Each new result was computed from scratch, without any attempt to generalisation [1] . We propose a general approach based on the recurrence relationships that the convolution functions satisfy.

In this paper we focus on the convolution surfaces obtained for skeleton given as a finite set of line segments, independently of the dimension of the ambient space. Line segments are the most fundamental 1-dimensional skeleton basic elements. We treat uniformly power inverse kernels and Cauchy type kernels in a very general way. The convolution functions obtained for higher order kernels are seen to be obtained from lower order ones through a recurrence of order 2. Similarly we introduce the recurrence for higher degree polynomial weights in terms of their lower degree and order counterparts.

It is not the intent of this paper to discuss the design or visualization of 3D shapes. The two dimensional graphics in the text are made to illustrate the mathematical purpose rather than impress. We invite the reader to look at the references in computer graphics to get a sense of beauty and variety of shapes that convolution surfaces allow. Yet our approach offers a way to produce and organize general reliable code for convolution surfaces.

[1] Except for Jin and Tai in (Section 3.5, 2002a) and (Section 5.2, 2002b).

So far, symbolic computation software were used to produce the necessary integration formulae on a case by case study. On one hand the recurrences we propose allow to produce all those formulae with a procedure of a few lines within a symbolic computation software. On the other hand we can use the code generation facilities provided by those systems to reliably produce efficient C implementation of the convolution functions to be easily incorporated in computer graphics software.

We furthermore exhibit the geometrical properties of convolution surfaces that are necessary in order to control the shape to be produced. In particular, we link the level set of a convolution function to the maximal and minimal thickness of the convolution surface.

In the first section we define kernels and convolution surfaces for curves and discuss their topological properties. In the second section we provide the recursive formulae for the convolution of line segments with a Cauchy and power inverse kernel. We then examine their geometrical properties. The case of polynomially weighted line segment is treated afterwards. At last we demonstrate how to reliably produce codes for insertion in computer graphics software.

2 Convolution surfaces

A convolution (hyper)-surface in $\mathbb{R}^n$ is the level set of a function that results from integrating a *kernel* function $\mathfrak{k}$ along a *skeleton* $\mathcal{S}$, which is a set of lower dimensional geometric elements: points, curves, polygons. The additivity property of integration allows superposition: we can concentrate in obtaining the convolution function for each single basic skeleton element. The convolution function for the whole skeleton is obtained by summing the convolution obtained for each of its elements. We define here the convolution function for a curve.

2.1 Notations

Typically $P = (p_1 \dots p_n)^T \in \mathbb{R}^n$ represents a point in space and $A = (a_1 \dots a_n)^T$, $B = (b_1 \dots b_n)^T$ represent the end points of a line segment $[AB]$. The straight line through A and B is noted (AB). Then $\overrightarrow{AP}$ represent the vector from A to P. In the following $\overrightarrow{u} = (u_1 \dots u_n)^T$, $\overrightarrow{v} = (v_1 \dots v_n)^T \in \mathbb{R}^n$ also represent vectors. The scalar product of two vectors $\overrightarrow{u} = (u_1 \dots u_n)^T$ and $\overrightarrow{v} = (v_1 \dots v_n) \in \mathbb{R}^n$ is then $\overrightarrow{u} \cdot \overrightarrow{v} = u_1 v_1 + \ldots + u_n v_n$. The distance between two points A and B is noted $|AB| = \sqrt{(b_1 - a_1)^2 + \ldots + (b_n - a_n)^2}$.

2.2 Kernels

The kernels in use in the literature are given by functions $\mathfrak{k} : \mathbb{R}^+ \to \mathbb{R}^+$. The argument is the distance between a point in space and a point on the skeleton. Those kernels are decreasing functions on $\mathbb{R}^+$ and strictly decreasing when non zero: $\mathfrak{k}(t) > 0 \Rightarrow \mathfrak{k}'(t) < 0$.

The first convolution surfaces to be used in computer graphics (Blinn, 1982; Bloomenthal and Shoemake, 1991) were based on the Gaussian kernel: $r \mapsto e^{-s\,r^2}$ that depends on a parameter $s > 0$. The difficulty in evaluating the resulting convolutions prompted the introduction of kernels that provided closed form convolution functions on basic skeletal elements. McCormack and Sherstyuk (1998); Sherstyuk (1999b) promoted the Cauchy kernel $r \mapsto \frac{1}{(1+s\,r^2)^2}$ after Wyvill and van Overveld (1996) introduced the inverse function $r \mapsto \frac{1}{r}$. For faster convolution Cani and Hornus (2001); Hornus et al. (2003) introduced the inverse cube kernel $r \mapsto \frac{1}{r^3}$. Jin and Tai (2002a) also exhibited the benefit of using the quintic inverse $r \mapsto \frac{1}{r^5}$.

In this paper we study the convolution of segments with Cauchy type and power inverse kernels:

$$\mathfrak{c}_s^i : r \mapsto \frac{1}{(1 + s\,r^2)^{\frac{i}{2}}} \qquad \text{and} \qquad \mathfrak{p}^i : r \mapsto \frac{1}{r^i}.$$

We shall establish that the resulting convolution functions satisfy a recurrence relationship of order two, bearing on i. We thus resort to the integration formulae for $i = 1$ and 2 only.

Gaussian, Cauchy and power inverse kernels decrease fast with distance but have an infinite support. Alternatively kernels with compact support, which are defined by piecewise polynomial functions, were also used (Nishimura et al., 1985; Wyvill et al., 1986; Sherstyuk, 1999b; Jin and Tai, 2002b; Jin et al., 2009). Those can avoid some unwanted blending but require more geometric computations.

2.3 One dimensional skeletons

We consider a bounded curve $\Gamma : [0, l] \subset \mathbb{R} \to \mathbb{R}^n$ parameterized by arc length. For a kernel $\mathfrak{k} : \mathbb{R}^+ \to \mathbb{R}^+$ the convolution function at a point $P \in \mathbb{R}^n$ is defined by

$$\mathcal{C}_\Gamma^{\mathfrak{g},\mathfrak{k}}(P) = \int_0^l \mathfrak{g}(s)\,\mathfrak{k}\left(|P\Gamma(s)|\right)\,\mathrm{d}s$$

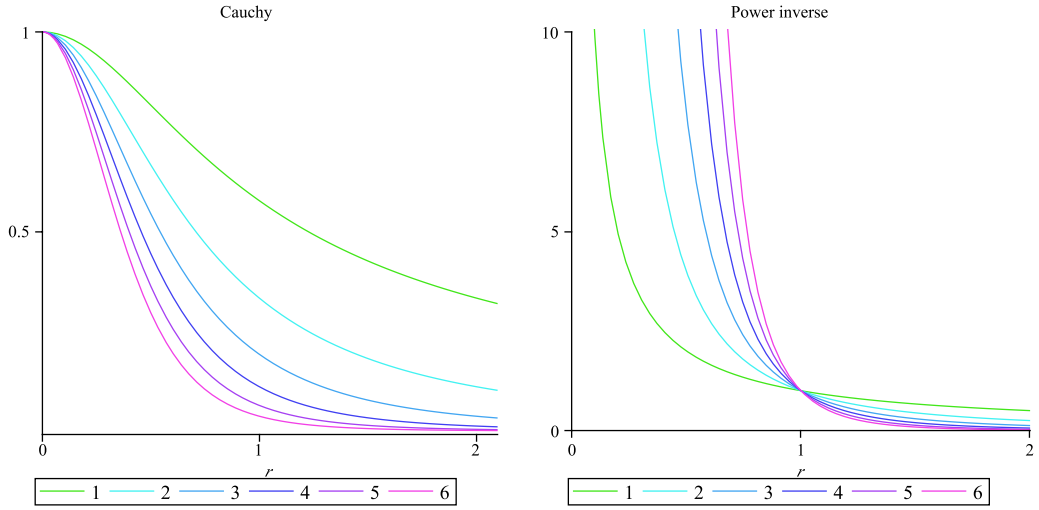

Fig. 1. Cauchy ($s = 2$) and power inverse kernels for different i

where $\mathfrak{g} : [0, l] \to \mathbb{R}$ is a *geometry function*. It is a continuous function on the skeleton that describes a *weight* that influences the shape of the convolution surface along the skeleton.

In a first step, $\mathfrak{g}(s) = 1$ and we shall write simply $\mathcal{C}_\Gamma^{\mathfrak{k}}$. At a second stage we consider a function that varies along the curve so as to have the thickness of the volume enclosed by the convolution surface evolve along the skeleton.

Proposition 2.1 *Assume that $\mathfrak{g}$ is continuous on $[0, l]$ and that, for all $s \in [0, l]$, $P \mapsto \mathfrak{k}(|P\Gamma(s)|)$ is k-time continuously differentiable in a domain $[a_1, b_1] \times \ldots \times [a_n, b_n]$ of $\mathbb{R}^n$. Then $\mathcal{C}_\Gamma^{\mathfrak{g},\mathfrak{k}}$ is k-time continuously differentiable on the interior of this domain.*

This comes from the Leibniz integral rule (see for instance Gasquet and Witomski (1999), Nickerson et al. (1959)) and actually entails that we can commute derivation and the integral sign.

Convolution functions obtained from a Cauchy kernel on a curve is therefore infinitely differentiable, while those obtained from a power inverse kernel are infinitely differentiable outside of the curve Γ.

As the reverse image of a closed set by a smooth map, the resulting convolution hyper-surfaces $\mathcal{C}_\Gamma^{\mathfrak{g},\mathfrak{k}}(P) = c$ are closed (in a topological sense) and smooth, provided c is not a critical value of $\mathcal{C}_\Gamma^{\mathfrak{g},\mathfrak{k}}$. It is the boundary of a smooth n-dimensional manifold V_c defined by $\mathcal{C}_\Gamma^{\mathfrak{g},\mathfrak{k}}(P) \geq c$. When $\mathfrak{g}$ is positive on $[0, l]$, V_c is compact [2]. Furthermore V_c and $V_{c'}$ are diffeomorphic provided that there

[2] Indeed, for any point at a distance greater than d to the curve $\mathcal{C}_\Gamma^{\mathfrak{g},\mathfrak{k}}(P) \leq \mathfrak{k}(d) \int_0^l g(s)\, ds$. Therefore V_c is bounded.

is no critical values in the interval $[c, c']$ (Milnor, 1963, Theorem 3.1).

Assuming the curve is piecewise regular, we can use any other parameterization $\Gamma : [a, b] \subset \mathbb{R} \to \mathbb{R}^n$ of the curve. The convolution function at a point $P \in \mathbb{R}^n$ is then defined by

$$\mathcal{C}_\Gamma^{\mathfrak{g},\mathfrak{k}}(P) = \int_a^b \mathfrak{g}(t)\, \mathfrak{k}\left(|P\Gamma(t)|\right)\, |\Gamma'(t)| \mathrm{d}t$$

where the function $\mathfrak{g}$ differs by the reparametrization.

3 Convolution of line segments

In this section we obtain the convolution functions resulting from the integration of the Cauchy and power inverse kernels along a line segment. The geometry function $\mathfrak{g}$ is constant and equal to 1. The formulae for such kernels of any order is obtained through a recurrence of order two. In the first paragraph we describe the parameterization we choose and exhibit the integral to be made explicit for both the Cauchy and power inverse kernels. In the second paragraph we provide the recurrence relationship that this integral satisfies. This leads then to the explicit recursive formulae for the convolution functions for both kernels.

3.1 Parameterization

The convolution functions obtained from integrating a Cauchy or power inverse kernel on a curve $\Gamma : [a, b] \to \mathbb{R}^n$ with constant weight function 1 are respectively given at $P \in \mathbb{R}^n$ by:

$$\mathfrak{C}_\Gamma^{0,i}(P) = \int_a^b \frac{|\Gamma'(t)|\, dt}{(1 + s|P\Gamma(t)|^2)^{\frac{i}{2}}} \quad \text{and} \quad \mathfrak{P}_\Gamma^{0,i}(P) = \int_a^b \frac{|\Gamma'(t)| dt}{|P\Gamma(t)|^i}$$

We consider here the case of a line segment $[AB]$. We use the parameterization $\Gamma : [0, 1] \to \mathbb{R}^n$ where $\Gamma(t) = A + t\,\overrightarrow{AB}$. We have $\Gamma'(t) = \overrightarrow{AB}$ and $|P\Gamma(t)|^2 = |AB|^2\, t^2 - 2\,\overrightarrow{AB} \cdot \overrightarrow{AP}\, t + |AP|^2$. The convolution functions are thus given by:

$$\mathfrak{C}_\Gamma^{0,i}(P) = |AB| \int_0^1 \frac{dt}{(s|AB|^2\, t^2 - 2\, s\, \overrightarrow{AB} \cdot \overrightarrow{AP}\, t + s\, |AP|^2 + 1)^{\frac{i}{2}}}$$

and

$$\mathfrak{P}_\Gamma^{0,i}(P) = |AB| \int_0^1 \frac{dt}{(|AB|^2 t^2 - 2\, \overrightarrow{AB} \cdot \overrightarrow{AP}\, t + |AP|^2)^{\frac{i}{2}}}.$$

The convolution of a line segment $[AB]$ with a Cauchy or a power inverse kernel thus boils down to integrating

$$\int_0^1 \frac{1}{(a\,t^2 - 2\,b\,t + c)^{\frac{i}{2}}} dt$$

for values of a, b, c depending on P but with the property $a > 0$ and $b^2 \leq a\,c$. The closed form formulae involve the quantities $a-2\,b+c$, $a-b$ and $\Delta = ac-b^2$. In the cases of interest here $\Delta \geq 0$.

For a *Cauchy kernel* we have:

$$a = s\,|AB|^2, \quad b = s\,\overrightarrow{AB} \cdot \overrightarrow{AP},\ c = s\,|AP|^2 + 1.$$

while $a-2\,b+c = s\,|BP|^2+1$, $\quad a-b = s\,\overrightarrow{BA}\cdot\overrightarrow{BP}$ and $\Delta = s\,|AB|^2(s\,|AP|^2+1) - s^2(\overrightarrow{AB} \cdot \overrightarrow{AP})^2$ is always strictly positive.

For a *power inverse kernel* we have:

$$a = |AB|^2, \quad b = \overrightarrow{AB} \cdot \overrightarrow{AP},\ c = |AP|^2$$

while $a-2\,b+c = |BP|^2$, $\quad a-b = \overrightarrow{BA}\cdot\overrightarrow{BP}$ and $\Delta = |AB|^2|AP|^2-(\overrightarrow{AB}\cdot\overrightarrow{AP})^2$. Note that $\Delta = |AB|^2|HP|^2$ where H is the orthogonal projection of P on the line (AB). Consequently $\Delta = 0$ when $P \in (AB)$.

3.2 Recurrences

In order to evaluate the convolution of a Cauchy or power inverse kernel on a segment we introduce the indefinite integral (primitive):

$$I_{0,i} = \int \frac{dt}{(a\,t^2 - 2\,b\,t + c)^{\frac{i}{2}}}$$

that depends on the order i of the kernel. Those integrals satisfy recurrence relationships (Prudnikov et al., 1986, 1.2.8.1 and 1.2.52.6) so that we can deduce $I_{0,i}$ for any $i \in \mathbb{Z}$ from the knowledge of $I_{0,1}$ and $I_{0,2}$ when $\Delta = ac - b^2 > 0$

We have

$$I_{0,1} = \frac{1}{\sqrt{a}} \ln\left(\frac{at - b}{\sqrt{a}} + (at^2 - 2\,bt + c)^{\frac{1}{2}}\right)$$

and

$$I_{0,2} = \frac{1}{\sqrt{ac - b^2}} \arctan\left(\frac{at - b}{\sqrt{ac - b^2}}\right)$$

Then for $i > 2$

$$(i-2)(c\,a - b^2)\,I_{0,i} + a\,(3-i)\,I_{0,i-2} = \frac{a\,t - b}{(a\,t^2 - 2\,b\,t + c)^{\frac{i-2}{2}}}. \tag{3.1}$$

The recurrence formula is obtained through integration by part or can be verified by differentiation. An open question in our sense is to determine those types of recurrences automatically.

The case $i = 3$ is easily deduced from this recurrence formula:

$$I_{0,3} = \frac{1}{c\,a - b^2}\frac{a\,t - b}{(a\,t^2 - 2\,b\,t + c)^{\frac{1}{2}}}.$$

This implies for an odd $i \geq 3$ the integral $I_{0,i}$ involves only radicals on top of arithmetic operations.

For the case $\Delta = ac - b^2 = 0$, which arises only for the power inverse kernels, we need to consider the relative value of $\frac{b}{a}$ with respect to the integration bounds. In this case $(at^2 - 2bt + c) = a(t - \frac{b}{a})^2$ and we thus need to evaluate $\int_0^1 \frac{dt}{a^{\frac{i}{2}}|t-\frac{b}{a}|^i}$. This integral is not properly defined when $0 \leq \frac{b}{a} \leq 1$. A case by case study when $b < 0$ or $b > a > 0$ leads us to the following formula:

$$\int_0^1 \frac{dt}{a^{\frac{i}{2}}|t - \frac{b}{a}|^i} = \begin{cases} \dfrac{1}{\sqrt{a}}\left|\ln\left(\dfrac{b-a}{b}\right)\right| & \text{if } i = 1 \text{ and } \frac{b}{a} \notin [0,1] \\ \dfrac{a^{\frac{i-2}{2}}}{i-1}\left|\dfrac{1}{|b-a|^{i-1}} - \dfrac{1}{|b|^{i-1}}\right| & \text{for } i > 1 \text{ and } \frac{b}{a} \notin [0,1] \end{cases}$$

3.3 Cauchy kernels

The convolution $\mathfrak{C}^{0,i}_{[AB]}$ generated by a segment $[AB]$ with constant weight function 1 and with a Cauchy kernel $\mathfrak{c}^i_s$ at a point $P \in \mathbb{R}^n$ is given, independently of the dimension, by the following formulae where $\Delta = s\,|AB|^2(s\,|AP|^2 + 1) - s^2\,(\overrightarrow{AB} \cdot \overrightarrow{AP})^2$.

$$\mathfrak{C}^{0,1}_{[AB]}(P) = \frac{1}{\sqrt{s}}\ln\left(\frac{|AB|(1+s|BP|^2)^{\frac{1}{2}} + \sqrt{s}\,\overrightarrow{BA}\cdot\overrightarrow{BP}}{|AB|(1+s|AP|^2)^{\frac{1}{2}} - \sqrt{s}\,\overrightarrow{AB}\cdot\overrightarrow{AP}}\right)$$

$$\mathfrak{C}^{0,2}_{[AB]}(P) = \frac{|AB|}{\sqrt{\Delta}}\left(\arctan\left(\frac{s\,\overrightarrow{BA}\cdot\overrightarrow{BP}}{\sqrt{\Delta}}\right) + \arctan\left(\frac{s\,\overrightarrow{AB}\cdot\overrightarrow{AP}}{\sqrt{\Delta}}\right)\right)$$

and for $i > 2$

$$\mathfrak{C}^{0,i}_{[AB]}(P) = \frac{s|AB|}{(i-2)\Delta}\left(|AB|\,(i-3)\,C^{0,i-2}_{[AB]}(P) + \frac{\overrightarrow{BA}\cdot\overrightarrow{BP}}{(1+s\,|BP|^2)^{\frac{i-2}{2}}} + \frac{\overrightarrow{AB}\cdot\overrightarrow{AP}}{(1+s\,|AP|^2)^{\frac{i-2}{2}}}\right).$$

The case $i = 3$ is easily deduced and involves only square roots beside arithmetic operations. Then for all higher odd i the convolution of the Cauchy kernel involves only algebraic functions.

The convolution hyper-surface is symmetric around the axis supporting the segment. It is therefore sufficient to visualize it in dimension 2. For a segment of length 1, we represent how the convolution surfaces $\mathfrak{C}^{0,3}(P) = c$ and $\mathfrak{C}^{0,4}(P) = c$ evolve with c, for $s = 1.8$.

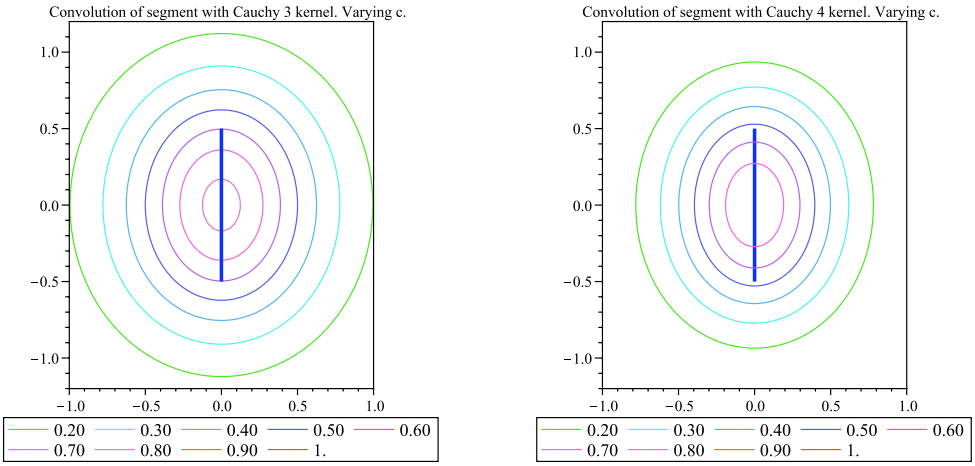

Fig. 2. Different level sets for the convolution function obtained for a fixed line segment with a Cauchy 3 (left) and 4 (right) kernel for $s = 1.8$.

3.4 Power inverse kernels

The convolution function $\mathfrak{P}^{0,i}_{[AB]}$ generated by a line segment $[AB]$ with a constant weight function 1 and with a power inverse kernel $\mathfrak{p}^i$ at a point $P \in \mathbb{R}^n$ are given, regardless of the dimension, by the following formulae, where $\Delta = |AB|^2|AP|^2 - (\overrightarrow{AB}\cdot\overrightarrow{AP})^2$.

$$\mathfrak{P}^{0,1}_{[AB]}(P) = \begin{cases} \left|\ln\left(\dfrac{|BP|}{|AP|}\right)\right| & \text{if } P \in (AB)\setminus\{A,B\} \\ \ln\left(\dfrac{|BA||BP| + \overrightarrow{BA}\cdot\overrightarrow{BP}}{|AB||AP| - \overrightarrow{AB}\cdot\overrightarrow{AP}}\right) & \text{otherwise} \end{cases}$$

$$\mathfrak{P}^{0,2}_{[AB]}(P) = \begin{cases} \infty & \text{if } P \in [AB] \\ \left| \dfrac{1}{|BP|} - \dfrac{1}{|AP|} \right| & \text{if } P \in (AB) \setminus [AB] \\ \frac{|AB|}{\sqrt{\Delta}} \left(\arctan\left(\dfrac{\overrightarrow{BA} \cdot \overrightarrow{BP}}{\sqrt{\Delta}} \right) + \arctan\left(\dfrac{\overrightarrow{AB} \cdot \overrightarrow{AP}}{\sqrt{\Delta}} \right) \right) & \text{otherwise} \end{cases}$$

and for $i > 2$

$$\mathfrak{P}^{0,i}_{[AB]}(P) = \begin{cases} \infty & \text{if } P \in [AB] \\ \dfrac{1}{i-1} \left| \dfrac{1}{|BP|^{i-1}} - \dfrac{1}{|AP|^{i-1}} \right| & \text{if } P \in (AB) \setminus [AB] \\ \dfrac{|AB|}{(i-2)\Delta} \left((i-3)\,|AB|\,\mathfrak{P}^{i-2}_{[AB]}(P) + \dfrac{\overrightarrow{BA} \cdot \overrightarrow{BP}}{|BP|^{i-2}} + \dfrac{\overrightarrow{AB} \cdot \overrightarrow{AP}}{|AP|^{i-2}} \right) & \text{otherwise} \end{cases}$$

In particular:

$$\mathfrak{P}^{0,3}_{[AB]}(P) = \begin{cases} \infty & \text{if } P \in [AB] \\ \dfrac{1}{2} \left| \dfrac{1}{|BP|^2} - \dfrac{1}{|AP|^2} \right| & \text{if } P \in (AB) \setminus [AB] \\ \dfrac{|AB|}{\Delta} \left(\dfrac{\overrightarrow{BA} \cdot \overrightarrow{BP}}{|BP|} + \dfrac{\overrightarrow{AB} \cdot \overrightarrow{AP}}{|AP|} \right) & \text{otherwise} \end{cases}$$

Note that though the integral underlying $\mathfrak{P}^{0,1}_{[AB]}$ is not properly defined for $P \in [AB]$ we see that $\mathfrak{P}^{0,1}_{[AB]}(P)$ converges to the announced value when P approaches the interior of the line segment.

Because of the symmetry around the straight line supporting the segment a 2D representation is quite sufficient for getting a sense of the shape of the convolution surface. We represent graphically how the convolution surface $\mathfrak{P}^{0,1}_{[AB]}(P) = c$, $\mathfrak{P}^{0,2}_{[AB]}(P) = c$ and $\mathfrak{P}^{0,3}_{[AB]}(P) = c$ evolve with c for a line segment of length 1.

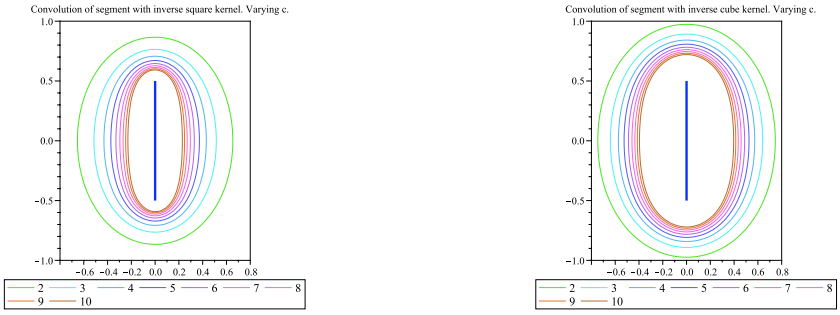

Fig. 3. Different level sets for the convolution function obtained for a fixed line segment with a square (left) and cubic (right) power inverse kernel.

4 Geometrical properties

As mentioned in Section 2.3 the convolution surfaces are bounded closed hyper-surfaces. The convolution surfaces are part of an algebraic surface when they are obtained through a Cauchy kernel $\mathfrak{c}_s^i$ or a power inverse kernel $\mathfrak{p}^i$ with i odd and bigger than 3.

As demonstrated in the pictures, the convolution surfaces generated by the Cauchy kernels need not enclose the whole segment. The convolution functions $\mathfrak{C}^{0,i}_{[AB]}$ are actually bounded and thus the convolution surface might be empty for a higher level set.

On the contrary, the functions $\mathfrak{P}^{0,i}_{[AB]}$, for $i \geq 2$, are unbounded. They tend to infinity as we approach the segment. Therefore all their (positive) level sets are non empty and enclose the segment $[AB]$. Furthermore, by increasing the value for the level set, the thickness decreases. This allows to thin down the convolution surface as much as needed along the segment.

We first derive the relationship between the level set c of a convolution surface $\mathcal{C}^{\mathfrak{k}}_{[AB]}(P) = c$ and the maximal thickness along the line segment. We then study separately the properties of the convolution surfaces obtained with a Cauchy kernel and those obtained with a power inverse kernel.

4.1 Maximal thickness around the segment

The first result applies to any convolution kernel $\mathfrak{k} : \mathbb{R}^+ \to \mathbb{R}^+$ that satisfies the hypothesis given in Section 2.2, namely $\mathfrak{k}$ is a decreasing functions on $\mathbb{R}^+$ and strictly decreasing when non zero: $\mathfrak{k}(t) > 0 \Rightarrow \mathfrak{k}'(t) < 0$. We then apply this result to obtain an implicit equation relating the maximal thickness along the segment of the convolution surface generated by the Cauchy and power inverse kernels.

Proposition 4.1 *The points of the hyper-surface $\mathcal{C}^{\mathfrak{k}}_{[AB]}(P) = c$, for $c > 0$, that are at maximal distance from (AB) are the points at equal distance from A and B.*

PROOF: The square of the distance of a point P to a point $M \in [AB]$ can be written as $|PM|^2 = |PH|^2 + |HM|^2$, where H is the orthogonal projection of P on (AB). Thus $r = |PH|$ is the distance of P to (AB). Take $\Gamma : t \in \mathbb{R} \mapsto A + t\overrightarrow{AB}$ for parameterization of (AB) and let $h \in \mathbb{R}$ be the coordinate of $H \in (AB)$. The points at equal distance from A and B are the points for which $h = \frac{1}{2}$.

Thus $\mathcal{C}^{\mathfrak{k}}_{[AB]}(P) = |AB| \int_0^1 \mathfrak{k}\left(r^2 + (t-h)^2\right)\, dt = G(r,h)$. For a point P to be on the level set c we need to have the relationship $G(r,h) = c$. This can be seen as an implicit function for r in terms of h. To find the greatest r for a given value of c, we look for critical points of this function:

$$\frac{\mathrm{d}r}{\mathrm{d}h} = -\frac{\partial G}{\partial h}\left(\frac{\partial G}{\partial r}\right)^{-1}$$

where

$$\frac{\partial G}{\partial h}(r,h) = \int_0^1 -\mathfrak{k}'\left(r^2 + (t-h)^2\right)\, 2\,(t-h)dt = -\int_{h^2}^{(1-h)^2} \mathfrak{k}'\left(r^2 + u\right)\, du.$$

We have $k' \leq 0$. If this latter integral vanishes because $\mathfrak{k}'(r^2 + (t-h)^2) = 0$ for almost every t then, due to our hypothesis on $\mathfrak{k}$, $\mathfrak{k}(r^2 + (t-h)^2) = 0$ for almost every t so that $\mathcal{C}^{\mathfrak{k}}_{\Gamma}(P) = 0$ and thus P cannot on the surface. This integral can thus only vanish when $(1-h)^2 = h^2$ i.e. $h = \frac{1}{2}$.

Since

$$\frac{\partial G}{\partial r}(r,h) = 2r \int_0^1 \mathfrak{k}'\left(r^2 + (t-h)^2\right) dt \leq 0$$

we furthermore deduce that, provided $r \neq 0$, $\dfrac{\mathrm{d}r}{\mathrm{d}h} > 0$ when $h < \frac{1}{2}$ and $\dfrac{\mathrm{d}r}{\mathrm{d}h} < 0$ when $h > \frac{1}{2}$. □

This proposition thus provides an equation linking the level set c and the maximal thickness τ achieved by the convolution surface $\mathcal{C}^{\mathfrak{k}}_{[AB]}(P) = c$. This relationship is obtained by evaluating the convolution function at the points on the perpendicular bisector to the line segment. We give the examples for the Cauchy kernel 3 and 4 and for the power inverse kernel 2 and 3.

The relationships between the thickness τ_i of the convolution surface $\mathfrak{C}^{0,i}_{[AB]}(P) = c$ obtained from a Cauchy kernel on a line segment of length l satisfies the re-

lationship

$$l \int_0^1 \frac{1}{\left(1 + s(\tau_i^2 + l^2(t - \frac{1}{2})^2)\right)^{\frac{i}{2}}} = c.$$

For instance, for $i = 3$ and 4 the relationship is:

$$\frac{l}{c} = (1 + s\tau_3^2)\sqrt{1 + s\left(\frac{l^2}{4} + \tau_3^2\right)}$$

and

$$c = \frac{l}{2(1 + s\tau^2)\left(1 + s\left(\frac{l^2}{4} + \tau_4^2\right)\right)} + \frac{1}{s^{\frac{1}{2}}(1 + s\tau_4^2)^{\frac{3}{2}}} \arctan\left(\frac{l}{2}\sqrt{\frac{s}{1 + s\tau_4^2}}\right).$$

We represent graphically this curve linking c and τ_i in Figure 4 for a varying length of the line segment, s being fixed to 1.8. The diamonds correspond to convolution surfaces touching the end points of the line segments. Level set for bigger values will not enclose the whole line segment. In agreement with what we observed earlier, there is a value of c beyond which the convolution surface is empty.

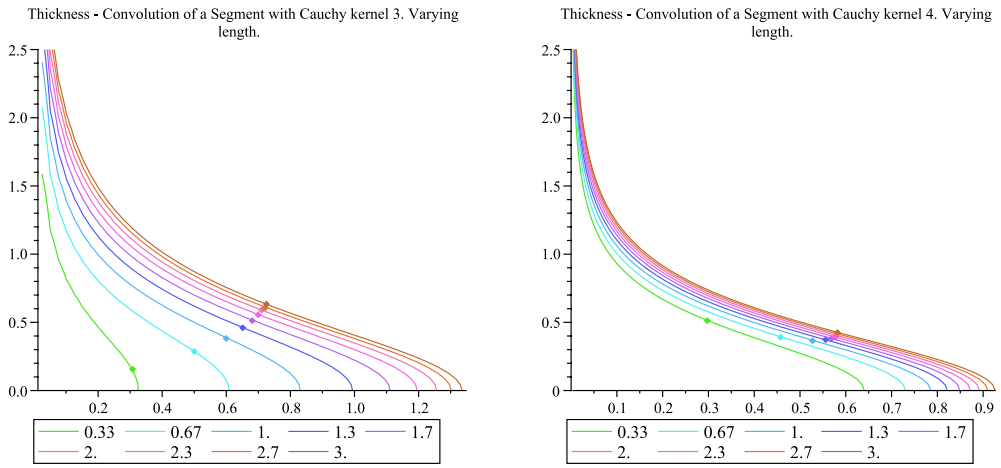

Fig. 4. Each curve represents the thickness of the convolution surface as a function of the level set. Different curves correspond to different lengths of the segment line. Cauchy 3 (left) and 4 (right) kernels were used. The diamonds correspond to convolution surfaces touching the end points of the line segments.

The relationships between the thickness τ_i of the convolution surface $\mathfrak{P}^{0,i}_{[AB]} = c$ obtained from a power inverse kernel on a line segment of length l satisfies the

relationship

$$l \int_0^1 \frac{1}{\left(\tau_i^2 + l^2(t-\frac{1}{2})^2\right)^{\frac{i}{2}}} = c.$$

For instance, for $i = 2$ and 3 the relationships are:

$$\frac{2}{\tau_2} \arctan\left(\frac{l}{2\,\tau_2}\right) = c \quad \text{and} \quad \tau_3^2 \sqrt{\frac{1}{4} + \frac{\tau_3^2}{l^2}} = \frac{1}{c}.$$

The graphic representation in Figure 5 of those relationship clearly shows that the convolution surface can be as thin as wished around the line segment.

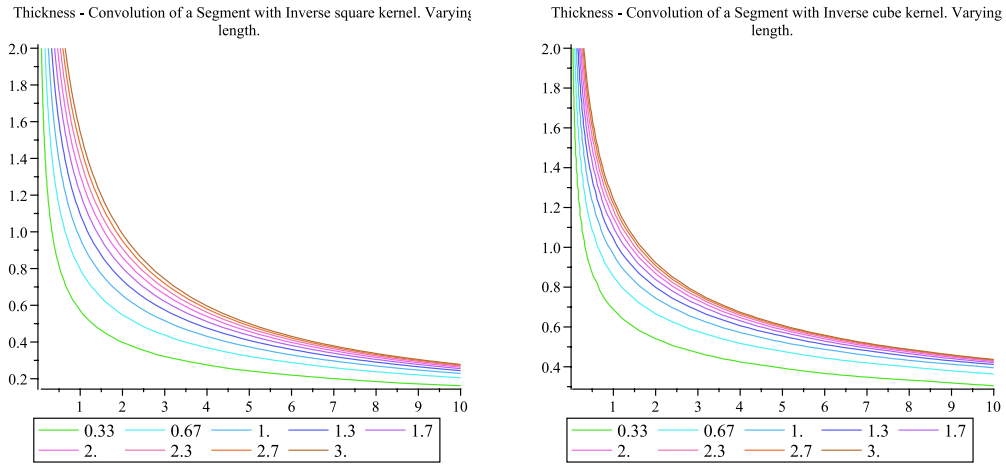

Fig. 5. Each curve represents the thickness of the convolution surface as a function of the level set. Different curves correspond to different lengths of the segment line. Left: inverse square kernel. Right: cubic inverse kernel.

4.2 Cauchy kernels

The convolution functions $\mathfrak{C}^{0,i}_{[AB]}$ obtained from a Cauchy kernel are well defined on all of $\mathbb{R}^n$, strictly positive, and bounded.

Proposition 4.2 *The function $P \to \mathfrak{C}^{0,i}_{[AB]}(P)$ increases as P approaches the mid point of the line segment $[AB]$ and reaches there a global maximum.*

PROOF: The convolution function $\mathfrak{C}^{0,i}_{[AB]}$ at P actually depends only on the distance r of P to the straight line (AB) and the position h of its orthogonal projection H on the line (AB):

$$\mathfrak{C}^{0,i}_{[AB]} = |AB| \int_0^1 \frac{dt}{(1 + s(|AB|^2(h-t)^2 + r^2))^{\frac{i}{2}}} = G(h,r).$$

We furthermore have

$$\frac{\partial G}{\partial r} = |AB| \int_0^1 \frac{-i\, sr\, dt}{(1 + s(|AB|^2(h-t)^2 + r^2))^{\frac{i+2}{2}}} \begin{cases} < 0 \text{ when } r > 0 \\ = 0 \text{ when } r = 0. \end{cases}$$

and

$$\frac{\partial G}{\partial h} = |AB|^3 \int_0^1 \frac{-i\, s\, (h-\ t)\, dt}{(1 + s(|AB|^2(h-t)^2 + r^2))^{\frac{i+2}{2}}}$$

$$= \frac{|AB|^3}{2} \int_{(h)^2}^{(1-h)^2} \frac{i\, s\, du}{(1 + s(r^2 + u))^{\frac{i+2}{2}}} = \begin{cases} < 0 \text{ when } h < \frac{1}{2} \\ = 0 \text{ when } h = \frac{1}{2} \\ > 0 \text{ when } h > \frac{1}{2}. \end{cases}$$

□

This maximum is the only critical value of $\mathfrak{C}^{0,i}_{[AB]}$. In accordance with Morse theory (Milnor, 1963) the topology of the convolution surface changes there. Above this value, the level sets are empty. More specifically for $i = 3, 4$:

$$\max_{\mathbb{R}^n} \mathfrak{C}^{0,3}_{[AB]} = \frac{2\,|AB|}{(4 + s|AB|^2)^{1/2}} \quad \text{and} \quad \max_{\mathbb{R}^n} \mathfrak{C}^{0,4}_{[AB]} = \frac{2\,|AB|}{4 + s\,|BA|^2} + \frac{1}{\sqrt{s}} \arctan\left(\frac{\sqrt{s}}{2}|BA|\right).$$

Another qualitative transition occurs when we take c greater than $\mathfrak{C}^{0,i}_{[AB]}(A) = \mathfrak{C}^{0,i}_{[AB]}(B)$. Then the volume $\mathfrak{C}^{0,i}_{[AB]}(P) \geq c$ does not contain the whole line segment. We therefore cannot slim down the convolution surface around the segment at will with a Cauchy kernel.

In explicit terms the convolution surface $C^{0,i}_{[AB]}(P) = c$ does not contain the whole line segment of length l for values of c above $\frac{l}{\sqrt{1+sl^2}}$ for $i = 3$ and $\frac{1}{2}\frac{l}{1+sl^2} + \frac{1}{2\sqrt{s}} \arctan(\sqrt{s}\, l)$ for $i = 4$.

4.3 Power inverse kernels

Proposition 4.3 *The convolution function $P \mapsto \mathfrak{P}^{0,i}_{[AB]}(P)$ increases as the distance of P to the line segment $[AB]$ decreases and is unbounded for $i > 1$.*

PROOF: The convolution function $\mathfrak{P}^{0,i}_{[AB]}$ at P actually depends only on the distance r of P to the straight line (AB) and the position h of its orthogonal projection H on the line (AB):

$$\mathfrak{P}^{0,i}_{[AB]} = |AB| \int_0^1 \frac{dt}{(|AB|^2(h-t)^2 + r^2)^{\frac{i}{2}}} = G(h, r)$$

For $0 \leq h \leq 1$ this function tends to $+\infty$ when r tends to zero.
We furthermore have

$$\frac{\partial G}{\partial r} = |AB| \int_0^1 \frac{-i\, r\, dt}{(|AB|^2(h-t)^2 + r^2)^{\frac{i+2}{2}}} < 0$$

and

$$\frac{\partial G}{\partial h} = |AB|^3 \int_0^1 \frac{-i\,(h-\,t)\, dt}{(|AB|^2(h-t)^2 + r^2)^{\frac{i}{2}}} \begin{cases} < 0 \text{ when } h > 1 \\ > 0 \text{ when } h < 0. \end{cases}$$

□

Proposition 4.4 *The minimal distance ρ from the convolution surface $\mathfrak{P}^{0,i}_{[AB]}(P) = c$, for $i > 1$, to the line segment $[AB]$ is reached on the line (AB) and satisfies the relationship*

$$\frac{1}{\rho^i} - \frac{1}{(l+\rho)^i} = c\,(i-1).$$

PROOF: In Proposition 4.1 we showed that the distance of a point P on the convolution surface $\mathfrak{P}^{0,i}_{[AB]}(P) = c$ to the line (AB) decreases as P drifts away from the perpendicular bisector hyperplane of the line segment $[AB]$. Using the parameterisation in the proof of this proposition, the distance of the points determined by (r, h) on the convolution surface to the line segment $[AB]$ is no longer r when $h < 0$ or $h > 1$. For those the distance to the line segment is given by the distance ρ to the end points, A or B respectively. We examine the situation around A.

We can write $|P\Gamma(t)|^2 = |AB|^2\, t^2 - 2\,\rho\,|AB|\cos(\alpha) + \rho^2$ where $\rho = |AP|$ and α is the angle between $\overrightarrow{AB}$ and $\overrightarrow{AP}$. Note that $\cos(\alpha) < 0$ when the projection of P on (AB) is outside of $[AB]$ on the opposite side of B from A.

The convolution function can thus be written

$$\mathfrak{P}^{0,i}_{[AB]}(P) = |AB| \int_0^1 \frac{dt}{(|AB|^2\, t^2 - 2\,\rho\,|AB|\cos(\alpha) + \rho^2)^{\frac{i}{2}}} = F(\rho, \alpha).$$

The points on the convolution surface satisfy $F(\rho, \alpha) = c$ which provides an implicit function for ρ in terms of α. We have $\frac{d\rho}{d\alpha} = -\frac{\partial F}{\partial \alpha}\left(\frac{\partial F}{\partial \rho}\right)^{-1}$ with

$$\frac{\partial F}{\partial \rho} = -i|AB| \int_0^1 \frac{(\rho - |AB|\cos(\alpha))dt}{(|AB|^2\, t^2 - 2\,\rho\,|AB|\cos(\alpha) + \rho^2)^{\frac{i+2}{2}}}$$

which is strictly negative in the case of interest and

$$\frac{\partial F}{\partial \alpha} = -i|AB|^2 \rho \sin(\alpha) \int_0^1 \frac{dt}{\left(|AB|^2\, t^2 - 2\,\rho\,|AB|\cos(\alpha) + \rho^2\right)^{\frac{i+2}{2}}}$$

which changes sign at $\alpha = 0$. The minimum of ρ as a function of α is thus reached for $\alpha = 0$, i.e. when P is on the straight line (AB). The formulae for $\mathfrak{P}^{0,i}_{[AB]}$ then provide us with the value of ρ at that point. □

4.4 Smoothness and sharpness

A convolution hyper-surface generated by a curve can be compared to a offset hypersurfaces to this curve. This latter is defined as the set of points away by a given distance d of the curve along the normal. The offset hypersurface generally presents cusps, even if the generating curve is smooth. On the contrary, the convolution hypersurface smoothes the generating curve. Figure 6 compares the offset line and convolution surface for three line segments. We used the thickness property demonstrated above to pick the appropriate level set of the convolution function.

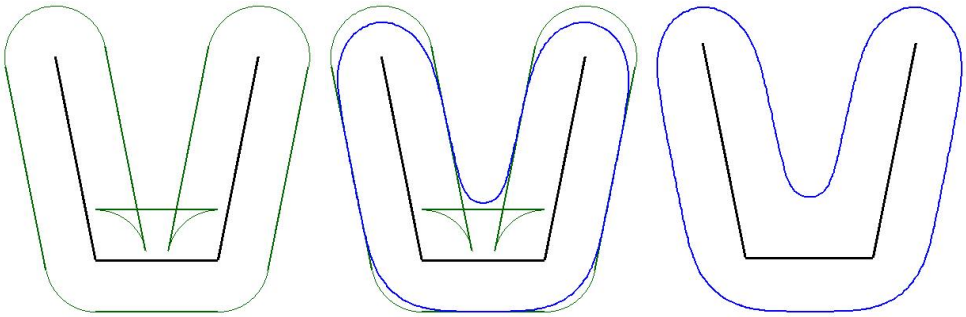

Fig. 6. Offset curves (left) and convolution curve (right) for a polygonal line.

One interesting aspect of having families of kernels then is the ability to increase the sharpness of the shape in the angles. Figure 7 shows the convolution surface generated by a set of 3, 4 and 5 line segments with power inverse kernels $i = 2, 4$ and 6. The level sets are adjusted thanks to the properties exibited above so that the tip of the branches have the same thickness. The recurrence formula then offers a mean of increasing the sharpness iteratively.

5 Weighted segments

Jin et al. (2001); Jin and Tai (2002a) introduced the formulae to modulate the convolution surface along a line segment according to a polynomial weight (or geometry function) up to degree 3. This allows to create tapered or inflated

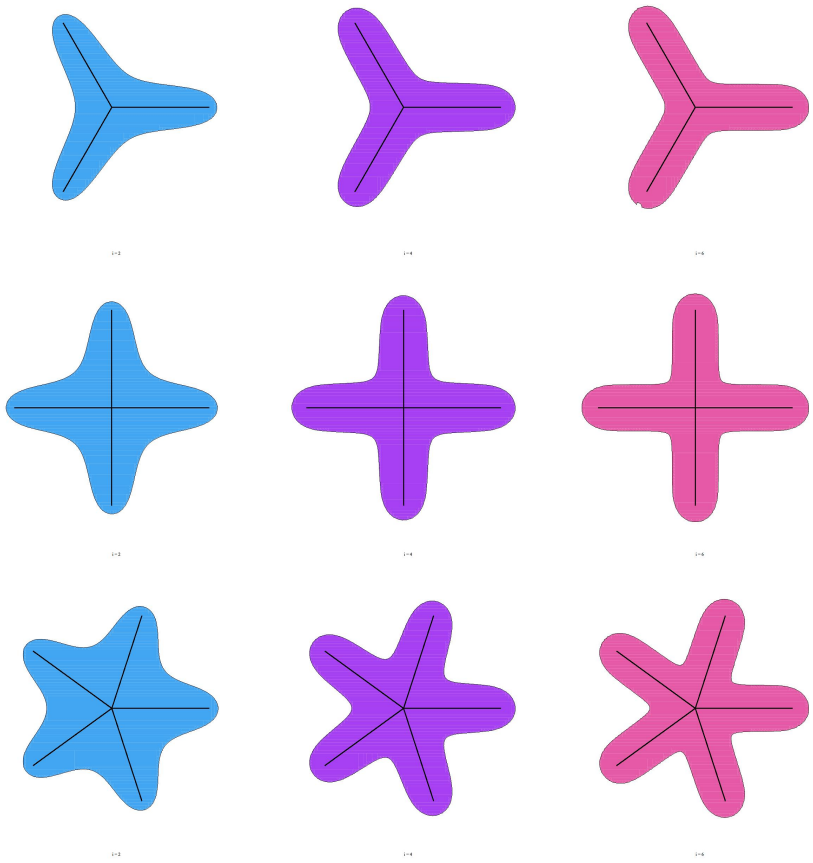

Fig. 7. Convolution curves for sets of 3, 4 and 5 line segments with power inverse kernels: left $i = 2$, middle $i = 4$, right $i = 6$.

shapes without subdividing the segment, which is the strategy proned by Hornus et al. (2003) with linearly varying weights. See Figure 8 that attempts a calligraphic feel to the Chinese character 2. We propose here a recursive formulation that allows to produce convolution functions for polynomial weight of any degree.

5.1 Parameterization

The geometry function $\mathfrak{g}$ that enters the definition function is now chosen as a polynomial function $\mathfrak{g} : t \mapsto w_0 + w_1 t + \ldots + w_k t^k$. Resuming the parameterization of Section 3.1, the convolution function is thus given by

$$\mathcal{C}^{\mathfrak{g},\mathfrak{k}}_{|AB|}(P) = |AB| \int_0^1 (w_0 + w_1\, t + \ldots + w_k t^k)\, \mathfrak{k}(|P\Gamma(t)|)\, dt.$$

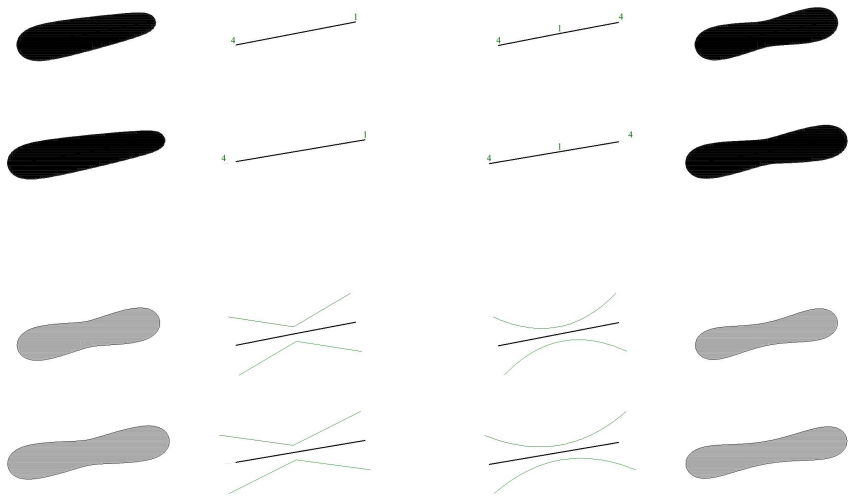

Fig. 8. One strategy to obtain a varying shape is to give weights to the vertices, and subdivide the line segment. This amounts to have piecewise linear geometry function on the line segment. Another strategy is to consider a geometry function that is given by a polynomial of higher degree.

For Cauchy and inverse power kernels, this boils down to evaluate the integrals

$$\int_0^1 \frac{t^k\,dt}{(at^2 - 2\,bt + c)^{\frac{i}{2}}}$$

for a, b, c as in Section 3.1

5.2 Recurrence

We shall evaluate the above integral recursively by applying the recurrence formulae on

$$I_{k,i} = \int \frac{t^k dt}{(a\,t^2 - 2\,b\,t + c)^{\frac{i}{2}}}$$

that can be found in (Prudnikov et al., 1986, p 47 and 102). They are obtained by integration by part or can be verified by differentiation.

The case $k = 0$ was treated in Section 3.2. For $k = 1$ we have:

$$I_{1,i} - \frac{b}{a} I_{0,i} = \begin{cases} \dfrac{1}{2a}\,\ln(a\,t^2 - 2\,b\,t + c) & \text{if } i = 2 \\ \dfrac{1}{a(2-i)}\,\dfrac{1}{(a\,t^2 - 2\,b\,t + c)^{\frac{i-2}{2}}} & \text{otherwise,} \end{cases}$$

while for $k \geq 2$ we shall distinguish the case where $k = i - 1$ from the case $k \neq i - 1$. We obtain:

$$a\, I_{i-1,i} - b\, I_{i-2,i} - I_{i-3,i-2} = \frac{1}{2-i} \frac{t^{i-2}}{(a\, t^2 - 2\, b\, t + c)^{\frac{i-2}{2}}}$$

and

$$a(i-k-1)\, I_{k,i} + b(2k-i)\, I_{k-1,i} - c(k-1)\, I_{k-2,i} = -\frac{t^{k-1}}{(a\, t^2 - 2\, b\, t + c)^{\frac{i-2}{2}}}.$$

5.2.1 Convolution functions

The recurrences above allow us to generate all the necessary convolution function for the Cauchy and power inverse kernels, for any order of the kernel, and any degree of the geometry function. We give here the recursive formula for the power inverse kernels. The one for the Cauchy kernels is obtained similarly but is just more cumbersome on paper.

We define

$$\mathfrak{P}^{k,i}_{[AB]}(P) = |AB| \int_0^1 \frac{t^k\, dt}{(|P(A + t\overrightarrow{AB})|)^i}.$$

Taking linear combinations, with coefficients $w_0, \ldots, w_d$, of those functions gives the desired convolution function for the weight function $t \mapsto w_0 + w_1 t + \ldots + w_k t^k$.

$$\mathfrak{P}^{k,i}_{[AB]}(P) = \begin{cases} \dfrac{\overrightarrow{AB} \cdot \overrightarrow{AP}}{|AB|^2}\, \mathfrak{P}^{0,2}_{[AB]}(P) + \dfrac{1}{|AB|} \ln\left(\dfrac{|BP|}{|AP|}\right) & \text{if } k = 1 \text{ and } i = 2 \\ \dfrac{\overrightarrow{AB} \cdot \overrightarrow{AP}}{|AB|^2}\, \mathfrak{P}^{0,i}_{[AB]}(P) + \dfrac{1}{(2-i)|AB|} \left(\dfrac{1}{|BP|^{i-2}} - \dfrac{1}{|AP|^{i-2}}\right) & \text{if } k = 1 \text{ and } i \neq 2 \\ \dfrac{\overrightarrow{AB} \cdot \overrightarrow{AP}}{|AB|^2}\, \mathfrak{P}^{i-2,i}_{[AB]}(P) + \dfrac{1}{|AB|^2}\, \mathfrak{P}^{i-3,i-2} + \dfrac{1}{(2-i)|AB|} \dfrac{1}{|BP|^{i-2}} & \text{if } k > 1 \text{ and } k = i - 1 \\ \dfrac{i-2k}{i-k-1} \dfrac{\overrightarrow{AB} \cdot \overrightarrow{AP}}{|AB|^2}\, \mathfrak{P}^{k-1,i}_{[AB]}(P) + \dfrac{k-1}{i-k-1} \dfrac{|AP|^2}{|AB|^2} \mathfrak{P}^{k-2,i}_{[AB]}(P) & \\ \quad - \dfrac{1}{|AB|(i-k-1)} \dfrac{1}{|BP|^{i-2}} & \text{otherwise} \end{cases}$$

5.2.2 Illustration

We show different shapes that can be obtained with polynomial weights. The skittle in Figure 5.2.2 can for instance be obtained with a degree 5 polynomial,

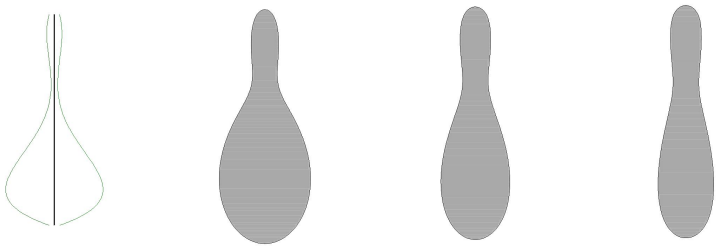

Fig. 9. Shape obtained with a geometry function of degree 5 and a power inverse kernel. From left to right: the skeleton and the geometry function, convolution for $i = 2$, for $i = 3$, for $i = 4$.

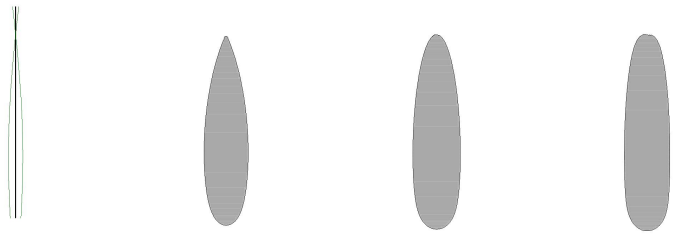

Fig. 10. Shape obtained with a geometry function that becomes negative on the top part of the line segment. From left to right: the skeleton and the geometry function, convolution for $i = 2$, for $i = 3$, for $i = 4$.

the graph of which is reprensented along the skeleton.

If the geometry function is negative, we might introduce a singular point, as is illustrated on Figure 10

In Figure 11 we sketch a more complex skeleton together with the graphs of the polynomial weights of degree up to 4 around it. On the right side we plot three level sets of the convolution function obtained with the cubic power inverse kernel and then with the quintic power inverse (the extra circles are artifacts of the plotting tool used, namely Maple). Thus obtained, each convolution curve is part of an algebraic curve.

The pictures of Figure 12 deptict some convolution surfaces created using the sketching system described by Bernhardt et al. (2008). The user paints a 2D region from which a geometric skeleton (defined as the locus of the centers of maximal discs included in the region) is computed. This skeleton is discretized into a set of segments along which the local desired radius is stored. A surface approximately fitting the region is then generated from the convolution of the Cauchy kernel along the segments. That motivates the need for finding precise correspondances between the level set and the resulting local thickness of the volume enclosed by the iso-surface. Once a shape is reconstructed, it can be blended with others, sketched from possibly different viewpoints and zoom factors.

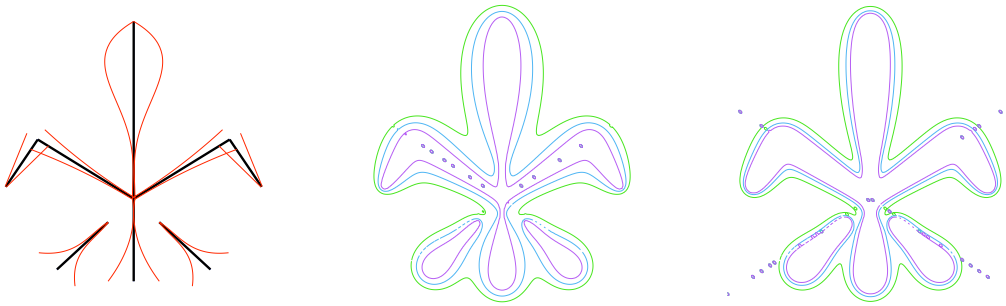

Fig. 11. On the left: skeleteton made of line segments with the graphs of the weight functions. Middle and right: different level sets for the convolution functions obtained with a cubic and quintic power inverse kernel.

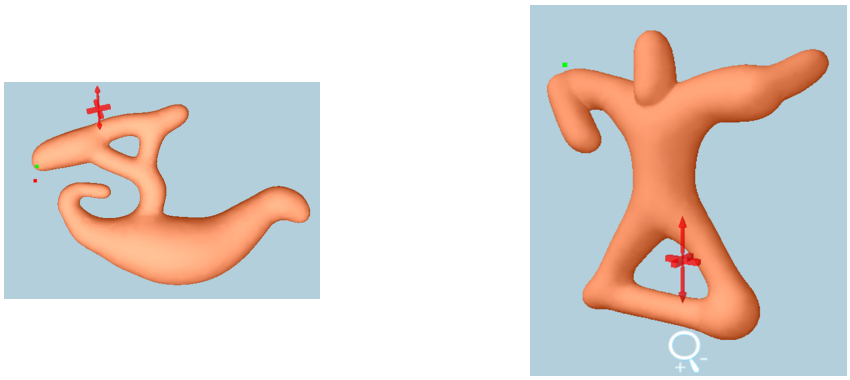

Fig. 12. Convolution surfaces created with the sketching system described in (Bernhardt et al., 2008).

6 Efficient and reliable production of code

One advantage of our recursive definition of the weighted convolution functions is that it allows the production of code (C, Java, Fortran) reliably and with little effort. On one hand the recursive definition of the polynomially weighted convolution functions we produced is easily implemented and checked in a computer algebra software. Then we can use the code generation capabilities of those systems to generate optimized code that can then be incorporated in computer graphics or rendering software.

We give here the complete Maple implementation of this idea for the kernel $r \mapsto \frac{1-s^4}{r} + \frac{s^4}{r}$ with polynomial weight of degree up to 3 suggested by Jin and Tai (2002a), s being a parameter to control sharpness. The reader can then appreciate how easy it is to have the code for his/her favorite kernel [3].

We first implement the Maple procedure `CP` that takes as parameter k, i and n that produces the formula of $\mathfrak{P}^{k,i}_{[AB]}(P)$ in dimension n.

```
vect  := (A,B,n) -> [seq(B[i]-A[i],i=1..n)]:
```

[3] We provide a file with this implementation on the web page `http://www-sop.inria.fr/members/Evelyne.Hubert/Publications`

```
scal  := (U,V,n) -> add(U[i]*V[i], i=1..n):
dist2 := (A,B,n) -> add((B[i]-A[i])^2, i=1..n);
dist  := (A,B,n) -> sqrt(dist2(A,B,n)):

CP := proc(k,i,n) local Delta;
  Delta := dist2(A,B,n)*dist2(A,P,n)-(scal(vect(A,B,n),vect(A,P,n),n))^2;
  if k = 0 then
    if i = 1 then
       ln(( dist(B,A,n)*dist(B,P,n)+scal(vect(B,A,n),vect(B,P,n),n))
          /(dist(A,B,n)*dist(A,P,n)-scal(vect(A,B,n),vect(A,P,n),n)));
    elif i = 2 then
       ( arctan( scal(vect(B,A,n),vect(B,P,n),n) /sqrt(Delta))
        + arctan(scal(vect(A,B,n),vect(A,P,n),n)/sqrt(Delta))
        ) *dist(A,B,n)/sqrt(Delta);
    else
       dist(A,B,n)/(i-2)/Delta*(
         (i-3)*dist(A,B,n)*CP(0,i-2,n)
         + scal(vect(B,A,n),vect(B,P,n),n)/dist(B,P,n)^(i-2)
         + scal(vect(A,B,n),vect(A,P,n),n)/dist(A,P,n)^(i-2));
    end if;
  elif k = 1 then
    if i=2 then
       scal(vect(A,B,n),vect(A,P,n),n)/dist2(A,B,n)*CP(0,2,n)
      + ln(dist(B,P,n)/dist(A,P,n))/dist(A,B,n);
    else
       scal(vect(A,B,n),vect(A,P,n),n)/dist2(A,B,n)*CP(0,i,n)
      + ((dist(B,P,n))^(2-i)-(dist(A,P,n))^(2-i))/dist(A,B,n)/(2-i);
    end if;
  elif k = i-1 then
      scal(vect(A,B,n),vect(A,P,n),n)/dist2(A,B,n)*CP(i-2,i)
     + CP(i-3,i-2,n)/dist2(A,B,n)+(dist(B,P,n))^(2-i)/(2-i)/dist(A,B,n)
  else
      (i-2*k)/(i-k-1)*scal(vect(A,B,n),vect(A,P,n),n)/dist2(A,B,n)*CP(k-1,i,n)
       + (k-1)/(i-k-1)*dist2(A,P,n)/dist2(A,B,n)*CP(k-2,i,n)
       - (dist(B,P,n))^(2-i)/dist(A,B,n)/(i-k-1) ;
  end if;
end proc:
```

Then creating the C code for the convolution function in dimension 2 of a segment $[AB]$ for polynomial weight of degree 3 and the kernel $r \mapsto \frac{1-s^4}{r} + \frac{s^4}{r}$ is obtained with the two command lines:

```
P1sP5 := unapply( add( w[k+1]*((1-s^4)*CP(k,1,2)+s^4*CP(k,5,2)),k=0..3),
        [w::'Vector'(4),s::float,A::'Vector'(2),B::'Vector'(2),P::'Vector'(2)]):
C(P1sP5, optimize,  deducetypes=false,  resultname="P1sP5");
```

The result is a C procedure that takes as parameter the array w of the four coefficients of the polynomial, the parameter s of the kernel, the arrays A and B representing the end points of the segment and finally the array P

representing the point at which the function needs to be evaluated.

```
#include <math.h>

double P1sP5 ( double w[4], double s, double A[2], double B[2], double P[2])
{
  double t1; [....] double t123;
  t2 = s*s; t3 = t2*t2;  t4 = 0.1e1-t3;
  t5 = B[0];  t6 = t5*t5;  t7 = A[0];  t10 = t7*t7;
  t11 = B[1];  t12 = t11*t11;  t13 = A[1];  t16 = t13*t13;
  t17 = t6-0.2e1*t5*t7+t10+t12-0.2e1*t11*t13+t16;
  t18 = sqrt(t17);  t19 = P[0];  t20 = t19*t19;
  t23 = P[1];  t24 = t23*t23;
  t27 = t20-0.2e1*t19*t5+t6+t24-0.2e1*t23*t11+t12;
  t28 = sqrt(t27);  t30 = t7-t5;  t32 = t30*(t19-t5);
  t33 = t13-t11;  t35 = t33*(t23-t11);
  t41 = t20-0.2e1*t19*t7+t10+t24-0.2e1*t23*t13+t16;
  t42 = sqrt(t41);  t44 = -t30;  t45 = t19-t7;
  t46 = t44*t45;  t47 = -t33;  t48 = t23-t13;  t49 = t47*t48;
  t53 = log((t18*t28+t32+t35)/(t18*t42-t46-t49));
  t56 = t44*t44;  t57 = t47*t47;  t58 = t56+t57;
  t59 = t45*t45;  t60 = t48*t48;  t61 = t59+t60;
  t63 = t46+t49;  t64 = t63*t63;  t68 = t32+t35;
  t66 = 0.1e1/(t58*t61-t64);
  t77 = 0.1e1/t28/t27;  t80 = 0.1e1/t42/t41;
  t82 = 0.2e1*t17*t66*(t68/t28+t63/t42)+t68*t77+t63*t80;
  t89 = 0.1e1/t58;  t90 = t63*t89;  t93 = 0.1e1/t18;
  t95 = t90*t53+(t28-t42)*t93;  t98 = t18*t66*t82;
  t103 = t90*t98/0.3e1-(t77-t80)*t93/0.3e1;
  t110 = t61*t89;  t113 = t28*t93;
  t115 = 0.3e1/0.2e1*t90*t95-t110*t53/0.2e1+t113/0.2e1;
  t121 = t77*t93;
  t123 = t90*t103/0.2e1+t110*t98/0.6e1-t121/0.2e1;
  return(  w[0]*(t4*t53+t3*t18*t66*t82/0.3e1)
          +w[1]*(t4*t95+t3*t103)
          +w[2]*(t4*t115+t3*t123)
          +w[3]*(t3*(-t90*t123+0.2e1*t110*t103-t121)
           +t4*(0.5e1/0.3e1*t90*t115-0.2e1/0.3e1*t110*t95+t113/0.3e1)));
}
```

7 Conclusion and perspectives

We reviewed and generalized the convolution functions for the most classical kernels - namely Cauchy and inverse powers - on line segments in a uniform way. We demonstrated how this allows to produce and organize code for computer graphics software efficiently and reliably from a symbolic computation

system.

The results and formulae are independent of the dimension. The need for dimension 2 and 3 is natural. Dimension 4 is also useful for a *lift and project* technique, currently under investigation, designed to avoid unwanted blending.

We are furthermore undertaking the present uniform recursive approach for convolution functions based on other basic skeleton elements. We are going to improve on McCormack and Sherstyuk (1998); Jin and Tai (2002b) by introducing weights on arcs of circles convolved with infinite support kernels. The case of planar polygons, previously treated in McCormack and Sherstyuk (1998); Jin et al. (2009), is also given an original treatment in Hubert (2010) that avoids the triangulation step and the difficult computation of the 2-dimensional integration domain in the case of compact support kernels. An open question in our sense is to determine the type of recurrence formulae needed automatically from the expression of the integral.

Acknowledgments : This research is part of the RTRA project and INRIA ARC PlantScan3D. We wish to thank B. Salvy and F. Chyzak for introducing us to Prudnikov et al. (1986) as well as J.B. Pomet, I. Kupka and D. Cohen-Steiner for discussions.

References

Angelidis, A., Cani, M.-P., 2002. Adaptive implicit modeling using subdivision curves and surfaces as skeletons. In: 7th Symposium on Solid Modeling and Applications. ACM, pp. 45–52.

Bernhardt, A., Pihuit, A., Cani, M.-P., Barthe, L., 2008. Matisse: Painting 2D regions for modeling free-form shapes. In: EUROGRAPHICS Workshop on Sketch-Based Interfaces and Modeling. pp. 57–64.

Blinn, J., 1982. A generalization of algebraic surface drawing. ACM Transactions on Graphics 1 (3), 235–256.

Bloomenthal, J., Shoemake, K., 1991. Convolution surfaces. Computer Graphics 25 (4), 251–255.

Bronstein, M., 2005. Symbolic integration. I, 2nd Edition. Vol. 1 of Algorithms and Computation in Mathematics. Springer-Verlag, Berlin.

Cani, M.-P., Hornus, S., 2001. Subdivision curve primitives: a new solution for interactive implicit modeling. In: International Conference on Shape Modeling and Applications. IEEE Computer Society Press, pp. 82–88.

Gasquet, C., Witomski, P., 1999. Fourier analysis and applications. Vol. 30 of Texts in Applied Mathematics. Springer-Verlag, New York.

Geddes, K. O., Czapor, S. R., Labahn, G., 1992. Algorithms for computer algebra. Kluwer Academic Publishers, Boston, MA.

Hornus, S., Angelidis, A., Cani, M.-P., 2003. Implicit modelling using subdivision curves. Visual Comput. 19 (2-3), 94–104.

Hubert, E., 2010. Convolution surfaces based on polygons for infinite and

compact support kernels. hal-inria (00429358), http://hal.inria.fr/inria-00429358/en/.

Jin, X., Tai, C.-L., 2002a. Analytical methods for polynomial weighted convolution surfaces with various kernels. Computers and Graphics 26, 437–447.

Jin, X., Tai, C.-L., 2002b. Convolution surfaces for arcs and quadratic curves with a varying kernel. The Visual Computer 18, 530–546.

Jin, X., Tai, C.-L., Feng, J., Peng, Q., 2001. Convolution surfaces for line skeletons with polynomial weight distributions. ACM Journal of Graphics Tools 6 (3), 17–28.

Jin, X., Tai, C.-L., Zhang, H., 2009. Implicit modeling from polygon soup using convolution. The Visual Computer 25 (3), 279–288.

McCormack, J., Sherstyuk, A., 1998. Creating and rendering convolution surfaces. The International Journal of the Eurographics Association, Computer Graphics Forum 17 (2), 113–120.

Milnor, J., 1963. Morse theory. Based on lecture notes by M. Spivak and R. Wells. Annals of Mathematics Studies, No. 51. Princeton University Press, Princeton, N.J.

Nickerson, H. K., Spencer, D. C., Steenrod, N. E., 1959. Advanced calculus. D. Van Nostrand Co., Inc., Toronto-Princeton, N.J.-New York-London.

Nishimura, H., Hirai, M., Kawai, T., Kawata, T., Shirakawa, I., Omura, K., 1985. Objects modeling by distribution function and a method of image generation (in japanese). The Transactions of the Institute of Electronics and Communication Engineers of Japan J68-D (4), 718–725.

Prudnikov, A. P., Brychkov, Y. A., Marichev, O. I., 1986. Integrals and series. Vol. 1. Gordon & Breach Science Publishers, New York.

Sherstyuk, A., 1999a. Interactive shape design with convolution surfaces. In: Shape Modeling International '99. pp. 56–65.

Sherstyuk, A., 1999b. Kernel functions in convolution surfaces: a comparative analysis. The Visual Computer 15 (4).

Wyvill, B., van Overveld, K., 1996. Tiling techniques for implicit skeletal models. SIGGRAPH Course Notes 11:1–26.

Wyvill, G., McPheeters, C., Wyvill, B., 1986. Data structure for soft objects. The Visual Computer 2 (4), 227–234.